Letter

Splitting of proton-antiproton directed flow in relativistic heavy-ion collisions

Piotr Bożek *

AGH University of Science and Technology, Faculty of Physics and Applied Computer Science, aleja Mickiewicza 30, 30-059 Krakow, Poland

(Received 18 July 2022; accepted 21 December 2022; published 27 December 2022)

The rapidity-dependent directed flow of particles produced in a relativistic heavy-ion collision can be generated in the hydrodynamic expansion of a tilted source. The asymmetry of the pressure leads to a buildup of a directed flow of matter with respect to the collision axis. The experimentally observed ordering of the directed flow of baryons, pions, and antibaryons can be described as resulting from the expansion of a baryon inhomogeneous fireball. An uneven distribution of baryons in the transverse plane leads to a difference in the collective push for protons and antiprotons. Precise measurements of the collective flow of identified particles as a function of rapidity could serve as a strong constraint on mechanism of baryon stopping in the early phase of the collision.

DOI: 10.1103/PhysRevC.106.L061901

The creation of a dense, strongly interacting matter in relativistic heavy-ion collisions manifests itself through the buildup of collective flow of emitted particles [1–3]. The collective flow reflects the gradient of the pressure in the fireball. The collective flow is parameterized using the harmonic flow coefficient for the azimuthal angle dependence of the observed spectra of produced particles. In particular, the directed flow with respect to the reaction plane Ψ_R is defined as a rapidity-dependent first harmonic coefficient $v_1(y)$

$$\frac{dN}{d\phi dy} = \frac{dN}{dy}[1 + 2v_1(y)\cos(\phi - \Psi_R) + \dots]. \quad (1)$$

In collisions of symmetric nuclei the directed flow is an odd function of rapidity.

The observation of the rapidity odd directed flow v_1 of charged particles produced in symmetric heavy-ion collisions [4–7] shows that the forward-backward symmetry is broken. In dynamic models of collisions it is due to an asymmetry of the initial conditions [8–20]. In noncentral collisions the initial state is expected to break the forward-backward symmetry. In the hydrodynamic model the directed flow can be explained by the expansion of a fireball tilted with respect to the collision axis [12]. This phenomenological model can describe the measured directed flow of charged particles. However, it cannot explain the observed splitting of the directed flow of identified particles [6,21]. In particular, the measured directed flow is different for protons and antiprotons, while in the hydrodynamic model particles of the same mass are expected to have a similar collective flow. Dynamical or hybrid models of heavy-ion collisions cannot explain the observed directed flow for identified particles at different energies [13,15,18,22–25]. Hybrid models using a cascade followed by a hydrodynamic model [15,26,27] predict a splitting in the final spectra, the directed, or the elliptic flow of baryons, antibaryons, and protons, without imposing a phase transition. However, no calculation exists that predicts the right ordering of the splitting of the rapidity-dependent directed flow of baryons, pions, and antibaryons at higher RHIC energies. For $\sqrt{s_{NN}} > 30$ GeV, effects of a possible phase transition are expected to be small, while the experiment shows a clear ordering (protons, pions, antiprotons) of the directed flow. This longstanding problem can be resolved assuming that the baryon distribution in the fireball is inhomogeneous. The baryon chemical potential is not only rapidity dependent [28], but also depends on the position in the transverse plane. The correlation between the position of the stopped baryon in the transverse plane and the position of the participant nucleon leads to a tilt of the baryon distribution. In the following, I show how this mechanism can explain the observed hierarchy of the directed flows of pions, protons, and antiprotons.

Dynamical models of the initial state are developed for the description of the creation and subsequent hydrodynamic evolution of a three-dimensional fireball in heavy-ion collisions [27,29–32]. In this Letter, the difference of the average flow of baryons, antibaryons, and pions is discussed. The effect on the average flow can be understood using a simple model with smooth initial conditions. The initial conditions are chosen in the form of a tilted fireball in the Glauber model [12]. The participant densities in the transverse plane (x, y) for the right $(+)$ and left $(-)$ going nuclei colliding at impact parameter b are

$$T_{\pm}(x, y) = A\, T(x \pm b/2, y)\big[1 - (1 - \sigma T(x \mp b/2, y))^A\big], \quad (2)$$

where

$$T(x, y) = \int dz \rho(\sqrt{x^2 + y^2 + z^2}), \quad (3)$$

ρ is the normalized nuclear density profile

$$\rho(r) = \frac{C}{1 + \exp[(r - R)/a]}, \quad (4)$$

*piotr.bozek@fis.agh.edu.pl

$\int d^3r\rho(r) = 1$. For the case studied in this letter, Au + Au collisions at $\sqrt{s_{NN}} = 200$ GeV, the parameters are $A = 197$, $\sigma = 42$ mb, $R = 6.37$ fm, $a = 0.54$ fm. The number of participant nucleons at impact parameter b is $N_{\rm part} = \int dxdy[T_+(x,y) + T_-(x,y)]$. The average multiplicity of produced particles is proportional to a combination $(1-\alpha)N_{\rm part} + 2\alpha N_{\rm coll}$, where the number of binary collisions $N_{\rm coll} = \sigma A^2 \int dxdyT(x+b/2,y)T(x+b/2,y)$. The three-dimensional distribution of the initial entropy density in the transverse plane and space-time rapidity $\eta_{||} = \frac{1}{2}\ln(\frac{t+z}{t-z})$ is

$$s(x,y,\eta_{||}) \propto [(1-\alpha)(T_+(x,y)f_+(\eta_s) + T_-(x,y)f_-(\eta_s)) + 2\alpha\sigma A^2 T(x+b/2,y)T(x+b/2,y)]H(\eta_{||}). \quad (5)$$

The two terms in the density correspond to the participant and binary collisions contributions to the overall multiplicity of produced particles. The longitudinal profile is

$$H(\eta_{||}) = \exp\left(-\theta\left(|\eta_{||}| - \eta_{||}^0\right)\frac{\left(|\eta_{||}| - \eta_S^0\right)^2}{2\sigma_\eta^2}\right), \quad (6)$$

with $\eta_{||}^0 = 1$ and $\sigma_\eta = 1.3$. The average entropy deposited in the interaction region by a participant nucleon is asymmetric in the longitudinal direction [11,33,34]. The corresponding profiles for left- and right-going participants are

$$f_\pm(\eta_{||}) = \begin{cases} 1, & \eta_{||} > \eta_T \\ \frac{\eta_T \pm \eta_{||}}{2\eta_T}, & -\eta_T \leqslant \eta_{||} \leqslant \eta_T \\ 0, & \eta_{||} < -\eta_T \end{cases}. \quad (7)$$

The linear form of the asymmetric profiles $f_\pm$ can describe the tilt of the fireball in the central rapidity region. Other *Ansätze* used [20,35] for the tilted fireball are very similar in this central rapidity region. The tilted fireball scenario has been successful is describing the observed charged particle directed flow [12]. The component of the initial density corresponding to the binary collision contribution is not tilted. The tilt of the fireball in the central region is determined by two parameters $\eta_T = 2.4$ and $\alpha = 0.1$. Please note that the asymmetric entropy deposition is an average description of of fluctuating string initial conditions [29,36]. The tilted and nontilted component reflects qualitatively the possibility of different kind of strings formed in the initial state, involving valence and see quarks from the participant nucleons.

The hydrodynamic expansion is performed using the three-dimensional version of the hydrodynamic code MUSIC [37–39] with shear viscosity $\eta/s = 0.08$ and an equation of state for quark-gluon plasma at finite baryon density [40]. The freeze-out takes place at the density $\epsilon_{fr} = 0.5$ GeV/fm^3. In a more realistic setup an earlier freezeout combined with a latter hadronic cascade stage could be used (ideally a hadronic cascade with a detailed balance between annihilation and creation of baryon-antibaryon pairs should be used). The effect of the hadronic stage on the directed flow is partly included in the calculation using an effective, delayed freezeout condition, but without hadronic afterburner. As long as both approaches reproduce the experimentally observed ratio of protons and antiprotons (or equivalently between transported and produced baryons), the predicted directed flow would be similar. Moreover, a possible change in the relative number a produced baryon due to annihilation, could change the magnitude of the splitting, but not the ordering in the predicted hierarchy of the slopes of the directed flow $\frac{v_1}{dy}$(antiprotons) < $\frac{dv_1}{dy}$(pions) < $\frac{dv_1}{dy}$(protons).

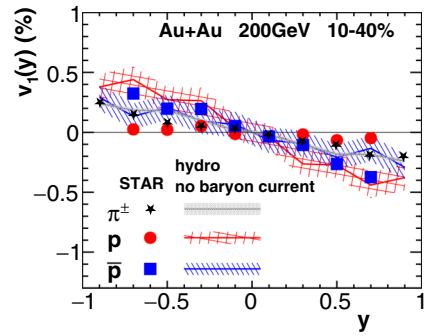

FIG. 1. Rapidity dependence of the directed flow of pions (stars and gray band), protons (full circles and red band), and antiprotons (squares and blue band) in 10–40 % centrality Au + Au collisions. The symbols represent the STAR Collaboration data [21] and the bands the results of the hydrodynamic expansion of a baryon homogeneous fireball.

In the very early stage of the collision a preequilibrium expansion is usually assumed. However, the existing implementations of the preequilibrium expansion use a two-dimensional, boost-invariant geometry [41]. Whereas, the early stage of the buildup of the directed flow is very sensitive to the relative values of the transverse and longitudinal effective pressures in the fluid [42]. In hybrid model calculations at energies $\sqrt{s_{NN}} \leqslant 27$ GeV it has been found that the directed flow can be generated already in the early hadronic phase of the dynamics [24]. The investigation of the details of such a very early three-dimensional evolution is beyond the scope of the present phenomenological study. Instead, a viscous hydrodynamic evolution is imposed from an early initialization time $0.2\,{\rm fm}/c$.

The expansion of the tilted fireball generates the rapidity-dependent directed flow. The model results reproduce reasonably well the directed flow of charged particles [12], but not the splitting of directed flows of protons and antiprotons [6,21]. The same kinematic cuts are used for pions and protons as in the experimental analysis. The directed flow of pions as a function of rapidity can be reproduced by the model using a tilted source initial conditions for the bulk of the matter (Fig. 1). In the calculation there is no baryon current and the flow of protons and antiprotons is similar. This is not surprising, as in this version of the hydrodynamic model the predicted flow depends only on the particle mass. The model cannot predict the observed splitting of the directed flow of baryons and antibaryons. At lower energies the splitting of baryon and antibaryon flow in hydrodynamic models could be related to a possible phase transition [15,18,23,24], to an effect of the spectator matter [43], or to the electromagnetic effect [44]. At the energy $\sqrt{s_{NN}} = 200$ GeV these effects

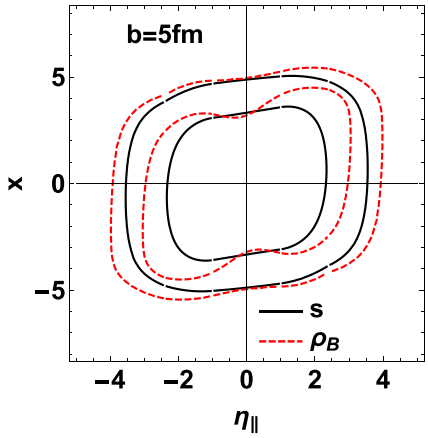

FIG. 2. Initial entropy density $s(x, 0, \eta_{||})$ (solid contours) and baryon density $\rho_b(x, 0, \eta_s)$ (dashed contours).

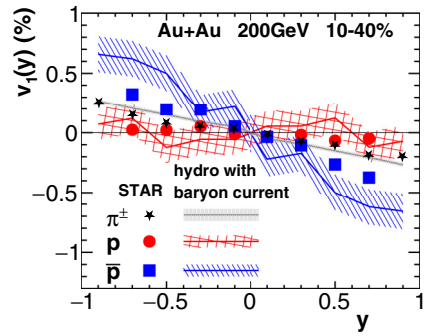

FIG. 3. Rapidity dependence of the directed flow of pions (stars and gray band), protons (full circles and red band), and antiprotons (squares and blue band) in 10–40 % centrality Au + Au collisions. The symbols represent the STAR Collaboration data [21] and the bands the results of the hydrodynamic calculation with baryon current.

cannot explain the observed splitting of directed flow. The baryon-antibaryon splitting of the directed flow indicates that the baryons transported from the initial colliding nuclei have effectively a different flow than the produced baryons and antibaryons [45].

In the hydrodynamic model the difference in the flow of baryons and antibaryons indicates that the net baryon density is finite and baryon currents are present in the expanding fireball. The initial baryon density is assumed to be of the form

$$\rho_B(x, y, \eta_{||}) \propto [(T_+(x, y)f_+(\eta_s) + T_-(x, y)f_-(\eta_s))] \times H(\eta_{||})H_B(\eta_{||}) \quad (8)$$

where $H_B(\eta_{||}) = \exp(-\frac{(\eta_{||}-\eta_b)^2}{2\sigma_B^2}) + \exp(-\frac{(\eta_{||}+\eta_b)^2}{2\sigma_B^2})$, with parameters $\eta_B = 4.4$ and $\sigma_B = 2.2$. The ratio of the transported and produced baryons at central rapidities [46] is reproduced with these initial conditions, which is essential for the description of the proton-antiproton splitting of directed flow. Please note, that the parametrization [Eq. (8)] of the baryon density is tilted with respect to the collision axis, but the tilt is slightly larger than for the bulk of the matter [Eq. (5)]. The *ansatz* used is phenomenological, but qualitatively justified in string models of the initial state [29,47,48]. The net baryon number transported to central rapidities must originate from the valence quarks in the participant nucleons. Therefore, the net baryon density in the transverse plane is strongly correlated to the density of participant nucleons. On the other hand, the deposited entropy is expected to originate from strings involving valence and sea quarks. This implies that the tilt of the initial entropy density could be smaller than the tilt of the initial baryon distribution. In Fig. 2 are shown the contour plots for the initial entropy and baryon number density distributions for a Au + Au collision at $b = 5fm$. The larger tilt of the initial baryon density generates inhomogeneities in the proton and antiproton distributions in the fireball. At positive space-time rapidities the proton density is larger in the upper part of the fireball on the figure, the reverse is true for the antiproton density.

The initial energy and baryon distributions are propagated using a viscous hydrodynamic evolution with baryon current using the MUSIC code. At the freezeout particles are emitted following the local temperature, flow velocity, and baryon chemical potential in a fluid cell, as well as shear viscosity corrections. As a result, the final proton directed flow of protons (antiprotons) is larger (smaller) than directed flow of pions at positive rapidities (Fig. 3). The model calculation reproduces well the rapidity-dependent directed flow for pions, similarly as for the calculation without baryon current (Fig. 1).

The tilt of the bulk of the fireball matter and the tilt of the baryon density change with the centrality of the collision. The slope of the rapidity dependence of the directed flow $dv_1(y)/dy$ is fitted in the central rapidity region $y \in [-1, 1]$ for each particle species at a range of centralities from 0%−70%. The result as a function of centrality is shown in Fig. 4 and compared to STAR Collaboration data. In semicentral collisions the model and the experimental data show the largest splitting between the slopes of the directed flow for the three particle species studied. The splitting is reduced for semiperipheral collisions in the experiment. Qualitatively this is also seen in the model calculation. The calculation is based on a phenomenological *ansatz*. The same phenomenological parameters determining the tilt of the fireball are used at all centralities and the experimental directed flow slopes for identified particles at different centralities are reproduced only qualitatively.

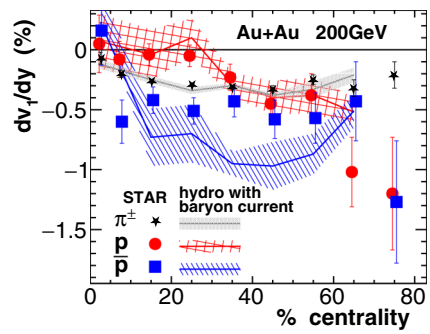

FIG. 4. The slope of the rapidity dependence of the directed flow of pions, protons, and antiprotons as function of centrality in Au + Au collisions. Symbols as in Fig. 3.

The analysis demonstrates the origin of the observed splitting of the baryon-antibaryon directed flow, but cannot replace microscopic models of the initial state. The directed flow of identified particles could serve as strong experimental constraint in the development of such realistic models of the initial state. The proposed mechanism could qualitatively explain the observed splitting of the baryon-antibaryon directed flow also at lower energies [21] (with adjusted parameters). Again, a detailed study of the energy dependence of the directed flow splitting should be rather based on more realistic models. For $\sqrt{s_{NN}} < 30$ GeV effects due to phase transition, shadowing by spectators or a mean field could also play a role.

This Letter presents a mechanism, which generates the splitting of the directed flow for protons and antiprotons in hydrodynamic models. This scenario strongly suggests that the distribution of baryons in the fireball is inhomogeneous in the transverse plane. This characteristic of the initial state could serve as a constraint for dynamical models of the initial state involving stopped baryons. This effect could have consequences for precise studies of the collective flow harmonics for identified particles or of the polarization for baryons and antibaryons [49,50]. The effects of splitting of the triangular v_3 or elliptic v_2 flow of protons, pions, and antiprotons at nonzero rapidity could also be studied. Similarly, other conserved charges could be unevenly distributed in the fireball. However, for strangeness the most important effect to be considered could be the different rate of strangeness saturation between the core and corona of the fireball and not the inhomogeneities of the net strangeness. Finally, let us note that a similar experimental and theoretical analysis could be performed for collision of asymmetric nuclei to gain additional information on the initial state of the hydrodynamic evolution.

This research is partly supported by the National Science Centre Grant No. 2018/29/B/ST2/00244.

[1] J.-Y. Ollitrault, J. Phys.: Conf. Ser. **312**, 012002 (2011).
[2] U. Heinz and R. Snellings, Annu. Rev. Nucl. Part. Sci. **63**, 123 (2013).
[3] C. Gale, S. Jeon, and B. Schenke, Int. J. Mod. Phys. A **28**, 1340011 (2013).
[4] A. Wetzler *et al.*, (NA49 Collaboration), Nucl. Phys. A **715**, 583c (2003).
[5] B. B. Back *et al.*, (PHOBOS Collaboration), Phys. Rev. Lett. **97**, 012301 (2006).
[6] L. Adamczyk *et al.*, (STAR Collaboration), Phys. Rev. Lett. **108**, 202301 (2012).
[7] B. I. Abelev *et al.*, (STAR Collaboration), Phys. Rev. Lett. **101**, 252301 (2008).
[8] L. P. Csernai and D. Rohrich, Phys. Lett. B **458**, 454 (1999).
[9] R. J. M. Snellings, H. Sorge, S. A. Voloshin, F. Q. Wang, and N. Xu, Phys. Rev. Lett. **84**, 2803 (2000).
[10] M. A. Lisa, U. W. Heinz, and U. A. Wiedemann, Phys. Lett. B **489**, 287 (2000).
[11] A. Adil and M. Gyulassy, Phys. Rev. C **72**, 034907 (2005).
[12] P. Bożek and I. Wyskiel, Phys. Rev. C **81**, 054902 (2010).
[13] J. Y. Chen, J. X. Zuo, X. Z. Cai, F. Liu, Y. G. Ma, and A. H. Tang, Phys. Rev. C **81**, 014904 (2010).
[14] L. P. Csernai, V. K. Magas, H. Stocker, and D. D. Strottman, Phys. Rev. C **84**, 024914 (2011).
[15] J. Steinheimer, J. Auvinen, H. Petersen, M. Bleicher, and H. Stöcker, Phys. Rev. C **89**, 054913 (2014).
[16] W. van der Schee and B. Schenke, Phys. Rev. C **92**, 064907 (2015).
[17] F. Becattini, G. Inghirami, V. Rolando, A. Beraudo, L. Del Zanna, A. De Pace, M. Nardi, G. Pagliara, and V. Chandra, Eur. Phys. J. C **75**, 406 (2015); **78**, 354 (2018).
[18] V. P. Konchakovski, W. Cassing, Y. B. Ivanov, and V. D. Toneev, Phys. Rev. C **90**, 014903 (2014).
[19] W. Ke, J. S. Moreland, J. E. Bernhard, and S. A. Bass, Phys. Rev. C **96**, 044912 (2017).
[20] Z.-F. Jiang, S. Cao, X.-Y. Wu, C. B. Yang, and B.-W. Zhang, Phys. Rev. C **105**, 034901 (2022).
[21] L. Adamczyk *et al.*, (STAR Collaboration), Phys. Rev. Lett. **112**, 162301 (2014).
[22] Y. Guo, F. Liu, and A. Tang, Phys. Rev. C **86**, 044901 (2012).
[23] Y. B. Ivanov and A. A. Soldatov, Phys. Rev. C **91**, 024915 (2015).
[24] Y. Nara, H. Niemi, A. Ohnishi, and H. Stöcker, Phys. Rev. C **94**, 034906 (2016).
[25] C.-Q. Guo, C.-J. Zhang, and J. Xu, Eur. Phys. J. A **53**, 233 (2017).
[26] J. Steinheimer, V. Koch, and M. Bleicher, Phys. Rev. C **86**, 044903 (2012).
[27] Y. Akamatsu, M. Asakawa, T. Hirano, M. Kitazawa, K. Morita, K. Murase, Y. Nara, C. Nonaka, and A. Ohnishi, Phys. Rev. C **98**, 024909 (2018).
[28] B. Biedron and W. Broniowski, Phys. Rev. C **75**, 054905 (2007).
[29] C. Shen and B. Schenke, Phys. Rev. C **97**, 024907 (2018).
[30] L. Du, U. Heinz, and G. Vujanovic, Nucl. Phys. A **982**, 407 (2019).
[31] C. Shen and B. Schenke, Phys. Rev. C **105**, 064905 (2022).
[32] A. De, J. I. Kapusta, M. Singh, and T. Welle, Phys. Rev. C **106**, 054906 (2022).
[33] S. J. Brodsky, J. F. Gunion, and J. H. Kuhn, Phys. Rev. Lett. **39**, 1120 (1977).
[34] A. Bialas and W. Czyż, Acta Phys. Polon. B **36**, 905 (2005).
[35] Z.-F. Jiang, S. Cao, W.-J. Xing, X.-Y. Wu, C. B. Yang, and B.-W. Zhang, Phys. Rev. C **105**, 054907 (2022).
[36] P. Bożek and W. Broniowski, Phys. Lett. B **752**, 206 (2016).
[37] B. Schenke, S. Jeon, and C. Gale, Phys. Rev. C **82**, 014903 (2010).
[38] B. Schenke, S. Jeon, and C. Gale, Phys. Rev. Lett. **106**, 042301 (2011).
[39] J.-F. Paquet, C. Shen, G. S. Denicol, M. Luzum, B. Schenke, S. Jeon, and C. Gale, Phys. Rev. C **93**, 044906 (2016).
[40] A. Monnai, B. Schenke, and C. Shen, Phys. Rev. C **100**, 024907 (2019).
[41] A. Kurkela, A. Mazeliauskas, J.-F. Paquet, S. Schlichting, and D. Teaney, Phys. Rev. C **99**, 034910 (2019).
[42] P. Bożek and I. Wyskiel-Piekarska, Phys. Rev. C **83**, 024910 (2011).
[43] C. Zhang, J. Chen, X. Luo, F. Liu, and Y. Nara, Phys. Rev. C **97**, 064913 (2018).

[44] A. Rybicki and A. Szczurek, Phys. Rev. C **87**, 054909 (2013).
[45] L. Adamczyk *et al.*, (STAR Collaboration), Phys. Rev. Lett. **120**, 062301 (2018).
[46] B. I. Abelev *et al.*, (STAR Collaboration), Phys. Rev. C **79**, 034909 (2009).
[47] A. Bialas and M. Jeżabek, Phys. Lett. B **590**, 233 (2004).
[48] M. Jeżabek and A. Rybicki, Eur. Phys. J. Plus **136**, 971 (2021).
[49] L. Adamczyk *et al.*, (STAR Collaboration), Nature (London) **548**, 62 (2017).
[50] X.-Y. Wu, C. Yi, G.-Y. Qin, and S. Pu, Phys. Rev. C **105**, 064909 (2022).